Hoop-Strong Nanotubes for Battery Electrodes

Khim Karki,[†] Yujie Zhu,[‡] Yihang Liu,[‡] Chuan-Fu Sun,[§] Liangbing Hu,[†] YuHuang Wang,[§] Chunsheng Wang,[‡,*] and John Cumings[†,*]

[†]Department of Materials Science and Engineering, University of Maryland, College Park, Maryland 20742, United States, [‡]Department of Chemical and Biomolecular Engineering, University of Maryland, College Park, Maryland 20742, United States, and [§]Department of Chemistry and Biochemistry, University of Maryland, College Park, Maryland 20742, United States

ABSTRACT The engineering of hollow nanostructures is a promising approach to addressing instabilities in silicon-based electrodes for lithium-ion batteries. Previous studies showed that a SiO_x coating on silicon nanotubes (SiNTs) could function as a constraining layer and enhance capacity retention in electrodes with low mass loading, but we show here that similarly produced electrodes having negligible SiO_x coating and significantly higher mass loading show relatively low capacity retention, fading quickly within the early cycles. We find that the SiNT performance can still be enhanced, even in electrodes with high mass loading, by the use of Ni functional coatings on the outer surface, leading to greatly enhanced capacity retention in a manner that could scale better to industrially relevant battery capacities. *In situ* transmission electron microscopy studies reveal that the Ni coatings suppress the Si wall from expanding outward, instead carrying the large hoop stress and forcing the Si to expand inward toward the hollow inner core. Evidence shows that these controlled volume changes in Ni-coated SiNTs, accompanied by the electrochemically inert nature of Ni coatings, unlike SiO_x, may enhance the stability of the electrolyte at the outer surface against forming a thick solid electrolyte interphase (SEI) layer. These results provide useful guidelines for designing nanostructured silicon electrodes for viable lithium-ion battery applications.

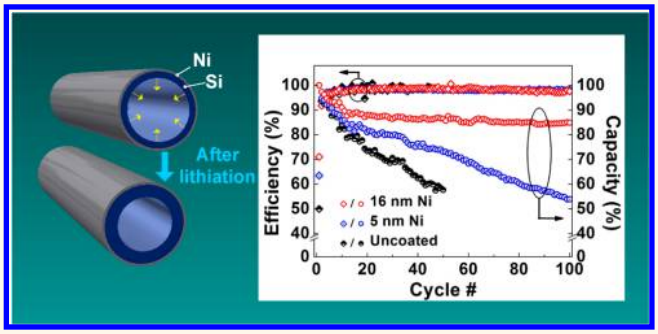

KEYWORDS: silicon nanotubes · nickel coating · SEI · *in situ* TEM · stability

Advanced lithium-ion battery technology has permeated the portable electronics industry and also has potential for application to electric vehicles and stationary grid storage.[1,2] Silicon is a promising candidate to replace current graphite anodes because it is an earth-abundant material with exceptional specific capacity of Li at room temperature (3579 *vs* 372 mAh/g for graphite).[2−4] However, silicon undergoes massive volume changes (~300%) during charge and discharge cycles leading to stress-induced cracking and poor cycle life.[5,6] To solve these problems and to move toward widespread industrial adoption of silicon-based lithium-ion batteries both require major improvements in three core areas: (i) structural integrity of the electrode, (ii) electronic and ionic transport pathways, and (iii) stability of the electrode/electrolyte interface. Nanostructured forms of silicon, particularly 1D structures, have been shown to mitigate some of the underlying problems observed in bulk counterparts.[7−13] For instance, the pioneering work by Chan *et al.* demonstrated nearly theoretical charge capacity in silicon nanowire (SiNW) anodes grown directly on a current collector.[8] The reduction in size and large surface-to-volume ratio of 1D nanowires facilitate lithiation-induced strain relaxation, short lithium diffusion lengths, and efficient electrical conducting pathways for faster charge and discharge cycles.

Unfortunately, the nanostructuring of silicon creates additional challenges due to the large surface-to-volume ratio, which leads to a large surface area that can cause unwanted side-reactions with the liquid electrolyte. For example, the reduction of organic electrolytes during the charge transfer process can lead to the formation of a solid electrolyte interphase (SEI) layer that reduces lithium diffusivity and causes irreversible capacity loss.[11] On the contrary, a thin SEI layer that only grows during the

* Address correspondence to cswang@umd.edu, cumings@umd.edu.

Received for review July 26, 2013 and accepted August 29, 2013.

Published online August 29, 2013
10.1021/nn403895h

initial few cycles can instead form a permanent protective layer preventing further growth, while allowing Li^+ ions to diffuse readily between the electrode and electrolyte. This variety of SEI is regarded as an ideal compromise for battery applications.[11,12] However, the notorious volume changes experienced by silicon during electrochemical cycling can simultaneously weaken and tear the SEI layer causing the silicon to be directly re-exposed to the electrolyte with each cycle, thus re-forming a new SEI film. This repeated reduction and consumption of electrolyte during cycling can quickly thicken the SEI layer, consuming lithium from cathodes and impeding the further transfer of Li^+ ions across the interface. This instability in SEI formation can eventually lead to overall capacity loss and failure of the battery.

Two main strategies have been implemented to stabilize and control the parasitic thickening of the SEI layers on nanostructured silicon electrodes. First, the use of functional coatings such as carbon,[9,14,15] copper,[16,17] nickel,[18,19] silver,[20] and alumina[21] on the surface of silicon electrodes has shown some promising outcomes. These surface coatings can act as a buffer layer between the active electrode and electrolyte and prevent the formation of excess SEI layers. Electronically active coatings also enhance the conducting pathways of the active Si and remove the need for extra additives.[4] Despite the advantages of such coatings, the precise role they play in constraining the volume changes in silicon during lithiation and delithiation is not fully understood. A second approach has focused instead on the internal structure of silicon nanomaterials, with the goal of providing stress relief through hollow nanostructures, with internal voids. Yao *et al.* compared the stress evolution during lithiation in a hollow nanosphere and a solid nanoparticle with the same volume of Si, and found that the solid form undergoes ~5 times more stress than the hollow counterpart.[22] Recent *in situ* transmission electron microscopy (TEM) studies on solid silicon nanostructures such as crystalline SiNWs[16] and amorphous Si nanorods[23] have demonstrated higher radial straining and simultaneous cracks in the structures when subjected to electrochemical lithiation and delithiation. Studies on corresponding hollow nanostructures, such as silicon nanotubes (SiNTs), have instead shown remarkable initial Coulombic efficiencies of >85% and stable capacity retention of >80% up through 50 cycles[9,10] These results all suggest that nanostructures with hollow or tubular shapes can provide substantial benefits over their solid counterparts.

Recently, one study combines the above two approaches, proposing the use of a 10 nm SiO_x coating as a mechanical clamping layer on the outer surface of a SiNT electrode, to prevent the outward expansion that can damage the SEI, and indeed, a coin cell using such a double-walled SiNT electrode showed excellent lithiation/delithiation cycle performance at a low Si mass loading (less than 0.1 mg/cm^2).[24] Inspired by this pioneering work, we seek to improve upon this approach by moving toward higher capacity battery electrodes with significantly increased mass loading, by 30−100 times, as would be required for a broader range of battery applications. By following the fabrication procedure published previously (see ref 24 and Experimental Methods section below), we can obtain SiNTs with only a very thin SiO_x coating—essentially uncoated nanotubes with only native oxide. When assembled into coin cells at the higher mass loading, these uncoated SiNTs show a rapid degradation of performance. To address this degradation, we additionally coat the outer surface of the SiNTs with nickel, which is both electronically conductive and inert to chemical interactions with lithium, like other metallic coatings,[16−20] and unlike SiO_x. We found that conductive, electrochemically inert Ni coating on SiNTs can address the above three challenges simultaneously: structure integrity, fast ion and electron transport, and stable SEI formation for electrodes with a large mass loading. We find that cell capacity-retention and cycle-life are improved with increasing thickness of the Ni-coating layers, suggesting that the high strength of the Ni coatings is indeed able to carry the large hoop stress caused by the expansion of the SiNTs during lithiation. To test such a hypothesis, we conduct further *in situ* TEM studies, and our observations confirm that, with the thicker Ni layers, the system exhibits a mode where the lithiation-induced expansion is in fact inward-directed entirely on the inner diameter and suppressed on the outer diameter.

RESULTS AND DISCUSSION

Electrochemical Performance of Uncoated SiNTs and Ni-Coated SiNTs. The electrochemical performances of uncoated SiNTs and Ni-coated SiNTs are tested under galvanostatic conditions in traditional liquid electrolyte coin cells with Li metal as the counter electrode (see Experimental Methods for details). Figure 1a shows schematics of SiNTs prepared by a carbon nanofiber nanotemplating method[24] (see Experimental Methods section for details). Three sets of SiNTs, one without any metallic coatings and the other two with sputter-coated Ni layers of different thicknesses prepared using direct current (DC)-magnetron sputtering (see Experimental Methods and Supporting Information, Figure S1 for details), are tested for the electrochemical performance. The free-standing uncoated SiNTs or Ni-coated SiNTs mats are directly used in cell assembly and electrochemical tests without using any binder and conductive additives (Figure 1b−f), as would be desired for maximum specific capacity in applications. Figure 1g shows the delithiation capacity retention of three electrodes with respect to the delithiation capacity of the first cycle. As shown in Figure 1g, after

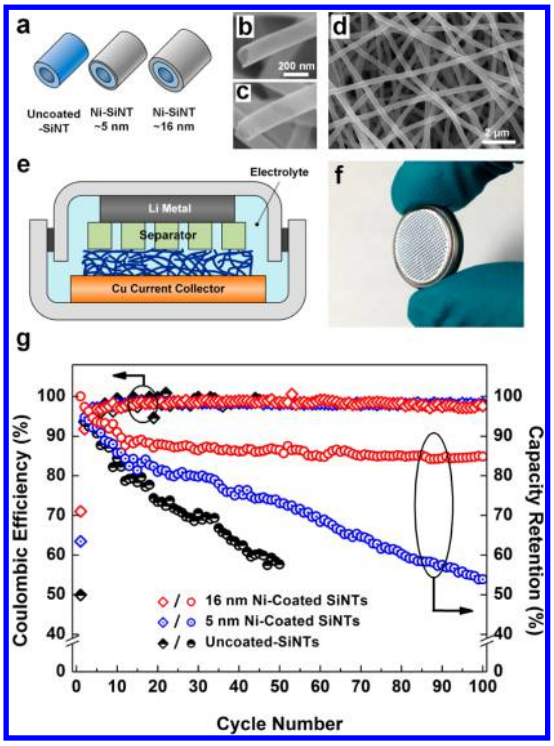

Figure 1. Electrochemical performance of uncoated SiNTs and Ni-coated SiNTs. (a) Schematics showing uncoated SiNT and SiNTs with Ni coating thicknesses of ~5 and ~16 nm (not to scale). Scanning electron microscopy (SEM) images of individual SiNTs (b) without Ni coating and (c) with ~16 nm Ni-coating. (d) A lower magnification SEM image of a SiNT mat prepared for coin-cell cycling. (e) A schematic of the coin-cell configuration with Li metal as counter electrode and SiNTs as working electrodes. (f) A representative coin-cell after assembly. (g) Curves showing Coulombic efficiency (CE) and capacity retention for uncoated SiNTs and SiNTs with Ni coating thicknesses of ~5 and ~16 nm. Compared to the uncoated SiNTs, adding Ni-coating layers improves the capacity retention of the cell for at least 100 cycles. Same scale bar in (b) and (c).

50 lithiation–delithiation cycles, the delithiation capacity of the uncoated SiNTs electrode quickly decreases to only ~55% of the first delithiation capacity. Although the ~5 nm Ni-coated SiNTs electrode shows slightly improved cycling performance compared with the uncoated SiNTs electrode, the capacity still fades during repeated cycling, with only 52% capacity left after 100 cycles. However, when the thickness of Ni-coating is increased to ~16 nm, the material shows excellent capacity retention with 85% capacity retained after 100 cycles. More importantly, almost no capacity decay is observed after the 20th charge–discharge cycle. Figure 1g clearly demonstrates that the ~16 nm Ni-coated SiNTs electrode shows superior cycling performance compared with the other two electrodes.

Detailed galvanostatic charge–discharge profiles are shown in Figure S2 (Supporting Information), where all three electrodes exhibit a long voltage plateau at ~200 mV (*vs* Li/Li^+) during the first lithiation, suggesting a two-phase lithiation mechanism in the first cycle, consistent with recent *in situ* TEM studies of amorphous silicon.[25,26] In the second and subsequent cycles, the voltage profiles show sloping curves, which are typical charge–discharge behaviors of amorphous silicon and indicate that the lithiation/delithiation follow a single phase solid solution reaction pathway. On the basis of the total weight of the electrode (active silicon with Ni coating) material, the first delithiation capacity and Coulombic efficiency (CE) of uncoated SiNTs are measured to be 930 $mAh/g_{electrode}$ and ~50% respectively. Similarly, the first discharge capacity and CE of ~5 nm Ni-coated SiNTs and ~16 nm Ni-coated SiNTs are 850 $mAh/g_{electrode}$ and ~63%, and 760 $mAh/g_{electrode}$ and ~71%, respectively. The overall specific capacity of two Ni-coated SiNT electrodes is slightly lower than that of the uncoated SiNT electrode, mainly due to the much higher mass density of Ni compared with amorphous Si. It is notable that the uncoated SiNTs achieve a discharge capacity of 930 mAh/g_{Si}, whereas the ~16 nm Ni-coated SiNTs achieve over 3000 mAh/g_{Si}, which shows that the Ni helps to maintain the mechanical and electronic integrity of the SiNT structure. We also note that the first-cycle CE is much lower for the uncoated SiNTs than that of ~5 nm Ni-coated SiNTs and ~16 nm Ni-coated SiNTs. This lower initial CE of uncoated SiNTs is probably caused by a large outward expansion of the SiNTs that breaks the SEI film during lithiation and delithiation, thus forming a thicker SEI layer that contributes to increasing cell impedance. On the other hand, the high CE in the Ni-coated SiNTs can be attributed to a stable SEI, resulting from the confinement of outward volume changes during lithiation and delithiation. To elucidate the origins of the different cycling behaviors of the above three electrodes, *in situ* TEM was used to directly observe all three electrodes during lithiation and delithiation cycling.

Lithiation and Delithiation Behavior of Individual Uncoated SiNTs. With the use of an *in situ* TEM platform, as reported in our previous studies,[27,28] a nanoelectrochemical cell comprising individual SiNTs, Li metal counter electrode and natively grown Li_2O electrolyte layer is constructed inside the TEM (Figure 2a). During the electrochemical cycling, a piezo-driven scanning tunneling microscopy (STM) tip carrying a Li metal source is brought in contact with the cantilevered end of the individual SiNT and a constant bias with respect to Li metal is applied to the nanotube. Figure 2b shows a representative uncoated SiNT, with its carbon core completely removed by the thermal oxidation process described in the Experimental Methods section. Figure 2c shows a side-view of such a SiNT with inner (d_{in}) and outer (d_{out}) diameters of ~213 and ~253 nm, respectively. Upon application of a constant bias with respect to Li metal (−4 V unless otherwise specified), Li propagates axially along SiNT, lithiating first on the outer surface of the wall followed by the

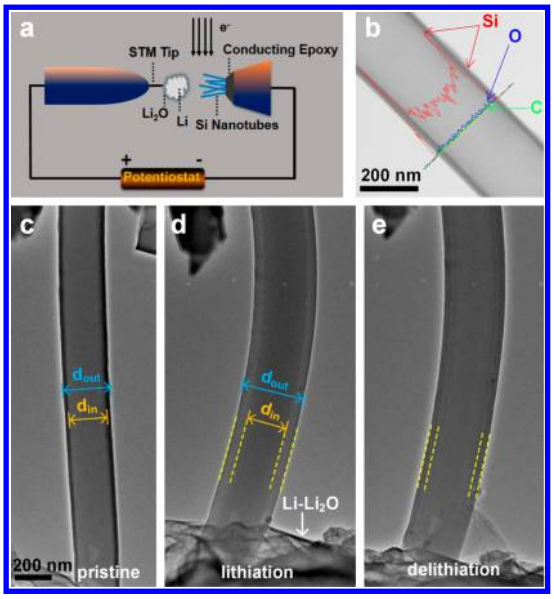

Figure 2. Lithiation and delithiation of an uncoated silicon nanotube (SiNT). (a) A schematic of nanoelectrochemical setup inside the TEM. (b) A representative energy dispersive X-ray spectroscopy (EDS) line profile scan across the SiNT shows strong Si peaks at the outer shell with little or no trace of C in the inner part. This demonstrates that the oxidation process has successfully removed the inner carbon core. (c) A pristine uncoated SiNT having inner diameter (d_{in}) ~213 nm and outer diameter (d_{out}) ~253 nm. (d) When we apply a bias of −4 V with respect to Li metal, SiNT undergoes lithiation with the following dimensional changes: d_{in} ~229 nm and d_{out} ~333 nm. (e) During delithiation, with biasing +4 V with respect to Li metal, the SiNT shrinks in size but does not reach to the pristine level. The d_{in} and d_{out} of the delithiated SiNT are ~227 and ~324 nm, respectively. Same scale bar (c−e).

inner core until it reaches the fully lithiated state (Figure 2d, see also Movie M1 in Supporting Information). After the SiNT is fully lithiated, the d_{in} and d_{out} are measured to be ~229 and ~333 nm, respectively, demonstrating an outward-radial volume expansion of ~210% and no inward expansion toward the core of the tube. It is notable that even the inner surface expands in the outward direction. As the reverse bias with respect to the Li metal is applied (+4 V unless otherwise specified), Li is extracted back, causing the SiNT to shrink (Figure 2e). The d_{in} and d_{out} of delithiated SiNT are measured to be ~227 and ~324 nm, respectively. This lithiation and delithiation process has been repeated on a number of similarly prepared SiNTs, all with quantitatively comparable results (Supporting Information, Figures S3 and S4).

Interestingly, a previous study with *post mortem* TEM[24] of similarly prepared SiNT structures showed indications of a strong constraining effect of a 10 nm thick thermally grown SiO_x surface layer, in which the silicon expanded only inwardly, toward the core, with no appreciable outward expansion during lithiation. However, no such constraining effect is observed with our electrochemical setup for our uncoated nanotubes, with only ~4 nm SiO_x coating. We note that the thickness of the SiO_x layer for the SiNTs we describe here is thinner than that reported in ref 24, although we used a similar fabrication procedure. This thin SiO_x apparently cannot force the SiNT to expand inward. We also point out that a number of studies conclude that SiO_x and other silicon oxides are not strictly inert to lithium,[29−32] and these chemical reactions of SiO_x with Li may alter its mechanical toughness. Further study is warranted to investigate the precise relationship between surface oxide composition and thickness to the lithiation- and delithiation-induced volume changes in SiNTs. However, this is beyond the scope of the present study. Instead, we choose to focus on a coating which is known to have high electron and Li ion mobility, yet is also inert against alloy formation and other insertion reactions. For this role, nickel presents an ideal model material with which to study the mechanical effects of a clamping layer independent of other electronic, ionic, or electrochemical considerations.[18,19]

Lithiation Behavior in Ni-Coated SiNTs. To evaluate the role of surface coatings in constraining the volume expansion of SiNTs during lithiation, we sputter-coat SiNTs with Ni using DC-magnetron sputtering (also see Supporting Information, Figure S1). Figure 3 shows *in situ* electrochemical cycling and simultaneous structural evolution observed during lithiation of Ni-coated SiNTs with various coating thicknesses of ~2, ~5, and ~16 nm (also see Supporting Information, Figure S5 and S6), together with schematics showing the expansion exhibited upon first lithiation of these structures (Figures 3b,c) and also the uncoated case (Figure 3a). First, we discuss the case of ~2 nm Ni thickness, as shown schematically in Figure 3b and in electron micrographs in Figures 3d−f. The d_{in} and d_{out} of as-prepared SiNTs, including the Ni-coating layers, are ~263 and ~324 nm, respectively (Figure 3d). Upon applying a constant bias with respect to Li metal, Li^+ ions diffuse into the silicon and propagate rapidly along the axis of the SiNT (Figure 3e). Notably, the lithiation follows two diffusion pathways on both the inner and outer surfaces of the SiNT,[28,33] which is evident as a tapered interface between the lithiated and unlithiated interface of the SiNT. The Li propagation is predominantly faster on the outer surface while proceeds at a slower rate in the inner core of the SiNT. The d_{in} and d_{out} of the fully lithiated SiNT are measured to be ~245 and ~380 nm, respectively, of which the outward radial expansion of d_{out} is only ~17%, relative to its initial value, whereas d_{in} now exhibits an *inward* expansion of ~7% (Figure 3f). The still outwardly directed overall expansion of the SiNT suggests that this relatively thin coating layer of nickel (~2 nm) is unable to constrain the volume changes experienced by SiNT during lithiation. However, it can be noted that it does result in some improvement in constraining the outer radial expansion, over the uncoated SiNTs (Figure 2).

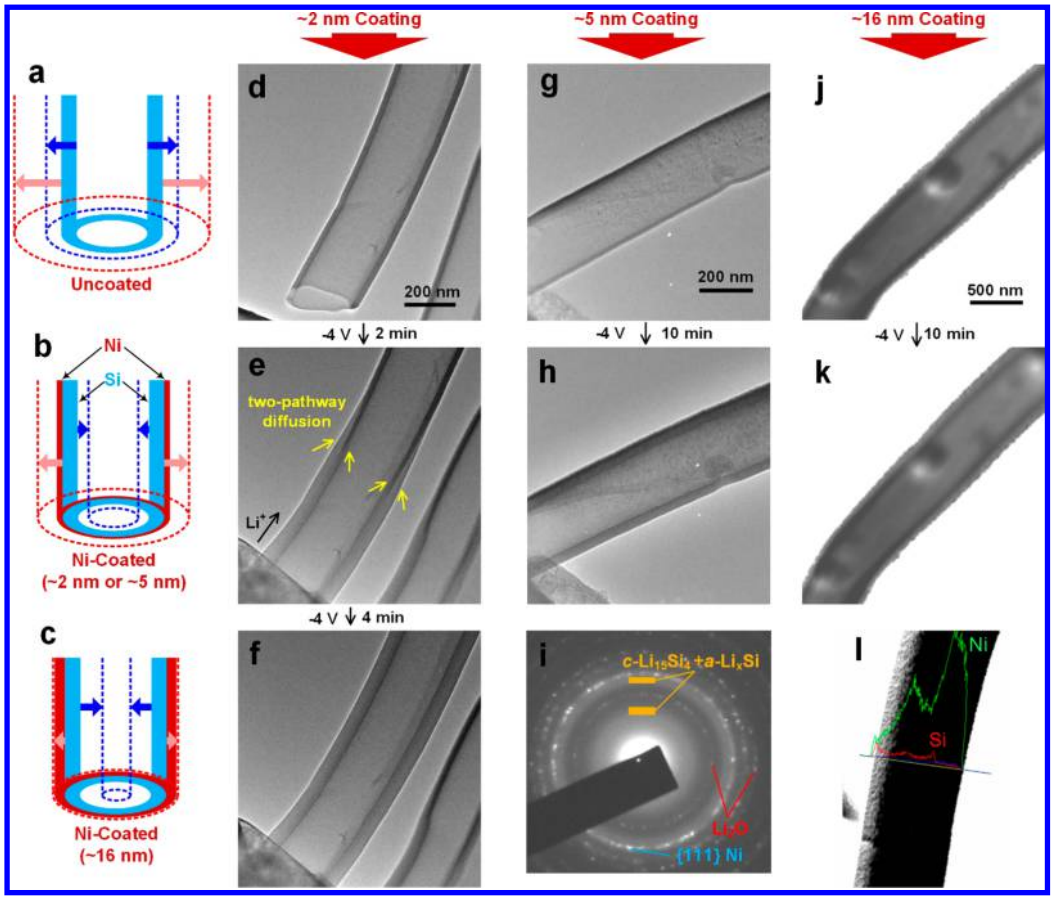

Figure 3. Comparison of lithiation behavior and simultaneous volume changes in SiNTs with different nickel coating thicknesses. (a−c) Schematics of uncoated SiNT and SiNT with nickel deposition thicknesses of ~2, ~5, and ~16 nm, as labeled (not to scale). The red and blue arrows show the direction and relative amount of expansion during the first lithiation of the outer diameter and inner diameter, respectively. (d) A ~2 nm Ni-coated SiNT with as-fabricated d_{in} ~263 nm and d_{out} ~324 nm. (e) As a bias of −4 V with respect to Li metal is applied to the SiNT, lithiation progresses axially following a two-pathway diffusion. The faster diffusion of lithium across the surface results in a tapered interface between the lithiated and unlithiated silicon. (f) A fully lithiated silicon with d_{in} ~245 nm and d_{out} ~380 nm. Although there is a considerable increase in d_{out}, the decrease in the d_{in} suggests that the Ni layer is constraining the outer expansion of silicon to some extent. Same scale bar (d−f). (g) SiNT with Ni coating of ~5 nm and as-fabricated d_{in} of ~218 nm and d_{out} of ~263 nm. (h) After lithiation, d_{in} and d_{out} are measured to be ~203 and ~290 nm, respectively. It is clear that there is lesser outer expansion and more toward the inner core as the thickness of the Ni coating is increased. Same scale bar (g and h). (i) An EDP image on the lithiated SiNT (h) shows the presence of polycrystalline $Li_{15}Si_4$ (*c*-$Li_{15}Si_4$), amorphous Li_xSi (*a*-Li_xSi), Li_2O and Ni. (j) SiNT with Ni coating of ~16 nm, d_{in} ~570 nm and d_{out} ~672 nm. (k) After lithiation, there was little change in the outer diameter (d_{out} ~678 nm) of the SiNT. The inner diameter shrank significantly (d_{in} ~521 nm). Same scale bar (j and k). (l) An EDS line scan profile across the SiNT shows strong Ni peaks compared to Si, indicating a thicker Ni coating.

Now, we turn to a discussion of ~5 nm Ni thickness samples, as shown schematically in Figure 3b and in electron micrographs in Figures 3g,h. The rougher surface texture of the as-prepared Ni-coated SiNTs is consistent with the grain growth of the thicker nickel film (Figure 3g). The measured d_{in} and d_{out} in the unlithiated state are measured to be ~218 and ~263 nm and changed to ~203 and ~290 nm after lithiation, respectively. Figure 3i shows an electron diffraction pattern of the lithiated SiNT shown in Figure 3h. The pattern indicates the presence of polycrystalline $Li_{15}Si_4$, Ni, Li_2O, and an amorphous Li_xSi phase (*a*-Li_xSi), consistent with previous studies.[28,34,35] When the Ni coating is increased from ~2 to ~5 nm, the outer radial expansion of the SiNT reduced from ~17% to ~10%, while the inward expansion (contraction) is maintained at ~7% during a similar reaction time. Moreover, no sign of surface cracks or Ni−Si interfacial debonding is observed during lithiation and delithiation, which suggest that any Ni deformation still occurs within the ductile limit. In core−shell nanostructures, material interfaces can sometimes serve as a nucleation site for cracking and delamination, due to compressive stress.[36] However, Si coatings on Ni have previously been shown to exhibit strong Ni−Si interfacial bonding even after hundreds of electrochemical cycles,[37] consistent with the results we report here.

Figure 3j,k shows the case of a relatively thick Ni coating layer of ~16 nm applied to the SiNT, yielding d_{in} and d_{out} that are measured to be ~570 and ~672 nm, respectively. An energy dispersive X-ray spectroscopy (EDS) line scan profile across a similar

TABLE 1. Summary of Relative Dimensional Changes of Silicon Nanotubes upon Lithiation[a]

Uncoated (% change)		Ni (~2 nm) (% change)		Ni (~5 nm) (% change)		Ni (~16 nm) (% change)	
Outer diameter	Inner diameter	Outer diameter	Inner diameter	Outer diameter	Inner diameter	Outer diameter	Inner diameter
35.7	9.0	17.3	-6.8	10.2	-6.9	0.9	-8.6
31.6	7.5	23.5	-6.6	9.5	-6.9	0.2	-18.8
26.3	4.7	20.6	-8.3	8.0	-4.3	0.2	-17.5

[a] The measured outer and inner diameters of uncoated SiNTs and Ni-coated SiNTs with different thicknesses before and after lithiation are given separately in Table S1 (Supporting Information).

nanotube shows higher peaks of Ni on the surface (Figure 3l), with only modest nonuniformity of Ni coating thickness. Figure 3k shows the same SiNT as Figure 3j after lithiation, and its measured d_{in} and d_{out} are found to be ~521 and ~678 nm, respectively. Here, the Si expands almost exclusively toward the inner core (~9% contraction of d_{in}), while relatively little expansion is seen on the outer surface of the nanotube (only ~1% increase in d_{out}). We also note that the two-pathway lithiation process, clearly observed in the case of ~2 nm coating, appears to be reduced to just the inner pathway for the ~16 nm case. This occurs in spite of the fact that Ni has been shown to have high Li mobility in other studies.[18,19] We observe that increasing the Ni coating thickness in fact blocks the outward volume expansion of the SiNT, simply because the hoop stress caused by this expansion is not able to overcome the tensile strength of the nickel coating layer. In the ~5 nm case, the two pathways proceed with similar ease due to the hoop stress, the outer pathway being constrained by the ductile expansion of Ni and the inner pathway by the SiNT itself.

Table 1 shows the summary of relative dimensional changes in the d_{in} and d_{out} of pristine and lithiated SiNTs with and without Ni coatings. The measured outer and inner diameters of uncoated SiNTs and Ni-coated SiNTs with different thicknesses before and after lithiation are given in Table S1 (Supporting Information). In the uncoated SiNTs, the expansion of the silicon wall during lithiation is primarily in the radially outward direction. There is no inward expansion toward the tubular core of SiNT. However, with additional surface coatings of SiNTs with Ni, the outer expansion of the silicon wall can be controlled. At ~2 nm of Ni coating, SiNTs undergo expansion both outwardly as well as inwardly, toward the core. The outer expansion is significantly constrained at ~5 nm of Ni coating, and going to ~16 nm produces a structure exhibiting almost no expansion on the outer surface, while much of the silicon expansion is forced inward toward the core. On the basis of the observations collected in Table 1, it is clear that Ni coatings can be beneficial in suppressing the lithiation-induced volume expansion in SiNTs. As Ni is a good electronic conductor, no conductive additives are needed, thereby lowering the size and weight of a cell, even though Ni is an inactive material for Li storage. From the comparative studies using different Ni coating thickness (Table 1), we estimated the optimum thickness of Ni coatings to be in the range of ~5−16 nm. We note that the coatings used here were applied using DC-magnetron sputtering, which, despite the high-porosity and transparency of the SINT mats, is still a somewhat directional process producing slight thickness nonuniformities. More efficient use of coating materials may be achieved through a more conformal technique such as atomic layer deposition (ALD) in future work. Furthermore, using stronger materials than Ni may be able to realize the same hoop-strong clamping mechanism with even thinner coatings.

CONCLUSIONS

Using *in situ* TEM studies, we directly observe the electrochemical lithiation/delithiation behavior and the nature of volume changes in individual SiNTs, both uncoated and with Ni coatings of different thickness. In uncoated SiNTs, the lithiation-induced volume expansion was predominantly in the outer radial direction, while no inward-directed expansion was observed. We find that the thickness of SiO_x grown by low temperature thermal oxidation (~4 nm at 500 °C) cannot sustain the huge stress produced by SiNT during lithiation. In Ni-coated SiNTs, the suppression of the outer volume expansion was readily achieved and improved as the thickness of the Ni coating layer was increased. We compare the electrochemical performance between uncoated SiNTs and SiNTs with ~5 and ~16 nm of Ni coatings, and we find that Ni-coated SiNTs demonstrate excellent initial CE and stable

capacity retention for at least 100 cycles. The presented results and associated analyses provide insightful guidelines for a viable design of hollow silicon nanostructures for lithium-ion battery applications.

EXPERIMENTAL METHODS

Preparation of Carbon Fibers. The SiNTs samples were prepared by a template method using carbon nanofibers.[24] The carbon nanofibers were prepared by an electrospinning method followed by carbonization. During the process, 1.0 g of polyacrylonitrile (PAN) (Sigma Aldrich) was added to 9.0 g of dimethyl formamide (DMF) (Sigma Aldrich) under mechanical stirring to form a viscous solution. The obtained viscous solution was transferred into a plastic syringe paired with a stainless steel needle (0.3 mm in diameter, *McMASTER-CARR*). The flow rate was kept at 6 μL/min. A grounded copper collector was used to collect the polymer fibers. A voltage of 15 kV was applied between the needle and the copper collector with the distance between them was kept at 15 cm. The as-collected polymer fibers were stabilized in air at a temperature of 280 °C for 5 h with a heating rate of 1 °C/min. The fibers were then precarbonized under argon atmosphere by heating to 500 °C with a heating rate of 10 °C/min and holding at this temperature for 0.5 h.

Silicon Nanotubes. Amorphous silicon was deposited on the carbon nanofibers by a low pressure chemical vapor deposition (LPCVD). The deposition parameters used were: 2 Torr of SiH_4 as the silicon source, 1 Torr of argon as the protective gas and at a temperature of 460 °C. The thickness of the silicon deposition was controlled by the growth time. Typically, a coat of ~25−30 nm was applied to the carbon fibers in 20−30 min. After silicon was coated onto the carbon nanofibers, the sample was heated in air at 500 °C for 2 h with a heating rate of 5 °C/min to remove the carbon core and form a SiO_x layer on the inner and outer surfaces of silicon nanotube. TEM-EDS line-scan analysis across the SiNT indicates that carbon has been completely removed during this oxidation process. During the thermal treatment, a SiO_x layer with modest thickness is expected to grow on the inner and outer surfaces of the SiNT. We determine the thicknesses of SiO_x layers to be ~4 nm by cross-sectional EFTEM (Supporting Information, Figure S1). We note that this thickness, while reproducible, is significantly below the 10 nm reported in ref 24 for a similar procedure. The ~4 nm thickness is only modestly higher than a room-temperature-formed native oxide layer (~2−3 nm), and this result can be attributed to the low processing temperature (500 °C) and short oxidation time (2 h), consistent with other results on the oxidation of bulk silicon.[38]

Ni Coating. A conformal Ni layer was coated on the silicon nanotubes by conventional DC-magnetron sputtering in an argon atmosphere (1 Pa) using a DC power density of 4.5 W cm^{-2}. The target-to-substrate distance was kept at 11 cm, and a single layer of Ni was coated at different deposition times of 10, 30, and 100 min.

Electrochemical Characterization. The free-standing uncoated SiNTs/Ni-coated SiNTs were directly used as electrodes for cell assembly without any binder and conductive additives. Coin cells, consisting of a uncoated SiNTs or Ni-coated SiNTs working electrode, a Li foil counter-electrode, Celgard 3501 microporous film separator, and 1.0 M $LiPF_6$ in ethylene carbonate (EC)/diethyl carbonate (DEC) (1:1 by volume) liquid electrolyte, were used for electrochemical tests. The active electrode mass loadings for uncoated-SiNTs and Ni-coated SiNTs were 3.6 and 3.3 mg/cm^2, respectively. Galvanostatic charge−discharge tests were performed by using an *Arbin BT 200* test station. Both cells were cycled between 0.01 and 1 V *vs* Li/Li^+ with a current density of 100 mA/g. The current density was calculated on the basis of the total weight of working electrode. After the cell reached the cutoff voltages, it was rested for 2 min before subsequent charge or discharge.

***In Situ* TEM Testing and Characterization.** *In situ* characterization was carried out using a JEOL JEM-2100 LaB_6 TEM operating at 200 kV. We use a specialized Nanofactory STM-TEM holder which simultaneously allows imaging and manipulation with three degrees of freedom in real-time. A prototype nanocell was prepared in a similar fashion as previously reported.[27,28] The samples comprising SiO_x-coated SiNTs and Ni-coated SiNTs were scraped from the substrate using a steel razor blade and glued separately to the Cu rod using conductive epoxy. The piezo-driven scanning tunneling microscope (STM) tip carried a fresh piece of Li metal, loaded in an inert environment, and which acts as a Li source as well as a counter electrode. The thin native Li_2O layer, which is formed on the surface of pristine Li metal inside the TEM due to residual gases (O_2 and H_2O) in the TEM column, serves as a solid-state electrolyte, allowing the diffusion of Li^+ between the electrodes under potential bias. Lithiation and delithiation were performed by applying a constant bias of −4 and +4 V, respectively.

Conflict of Interest: The authors declare no competing financial interest.

Acknowledgment. We thank X. Zhang and R. Briber for help with the microtome. This work was initiated and supported as part of Nanostructures for Electrical Energy Storage (NEES), an Energy Frontier Research Center funded by the U.S. Department of Energy, Office of Science, Office of Basic Energy Sciences under Award Number DESC0001160. The support of the Maryland NanoCenter and shared experimental facilities support from the NSF MRSEC under Grant DMR 05-20471 are gratefully acknowledged.

Supporting Information Available: Further details on the surface coating thickness measurements for different SiNTs (Figure S1), galvanostatic charge/discharge profile (Figure S2), additional *in situ* TEM lithiation and delithiation experiments (Figure S3−S6), measured outer and inner diameters of different SiNT samples studied (Table S2), and a movie showing *in situ* TEM lithiation of an uncoated SiNT (Movie M1). This material is available free of charge *via* the Internet at http://pubs.acs.org.

REFERENCES AND NOTES

1. Armand, M.; Tarascon, J. M. Building Better Batteries. *Nature* **2008**, *451*, 652–657.
2. Aricò, A. S.; Bruce, P.; Scrosati, B.; Tarascon, J. Schalkwijk. Nanostructured Materials for Advanced Energy Conversion and Storage Devices. *Nature* **2005**, *4*, 366–377.
3. Obravac, M. N.; Christensen, L. Structural Changes in Silicon Anodes during Lithium Insertion/Extraction. *Electrochem. Solid-State Lett.* **2004**, *7*, A93–A96.
4. Kasavajjula, U.; Wang, C.; Appleby, A. J. Nano- and Bulk-Silicon-Based Insertion Anodes for Lithium-Ion Secondary Cells. *J. Power Sources* **2007**, *163*, 1003–1039.
5. Christensen, J.; Newman, J. Stress Generation and Fracture in Lithium Insertion Materials. *J. Solid State Electrochem.* **2006**, *10*, 293–319.
6. Sethuraman, V. A.; Chon, M. J.; Shimshak, M.; Srinivasan, V.; Guduru, P. R. *In-situ* Measurements of Stress Evolution in Silicon Thin Films During Electrochemical Lithiation and Delithiation. *J. Power Sources* **2010**, *195*, 5062–5066.
7. Takamura, T.; Ohara, S.; Uehara, M.; Suzuki, J.; Sekine, K. A Vacuum Deposited Si Film Having a Li Extraction Capacity over 2000 mAh/g with a Long Cycle Life. *J. Power Sources* **2004**, *129*, 96–100.
8. Chan, C. K.; Peng, H.; Liu, G.; McIlwrath, K.; Zhang, X. F.; Huggins, R. A.; Cui, Y. High-Performance Lithium Battery Anodes Using Silicon Nanowires. *Nat. Nanotechnol.* **2008**, *3*, 31–35.
9. Park, M.; Kim, M. G.; Joo, J.; Kim, K.; Kim, J.; Ahn, S.; Cui, Y.; Cho, J. Silicon Nanotube Battery Anodes. *Nano Lett.* **2009**, *9*, 3844–3847.

10. Song, T.; Xia, J. L.; Lee, J. H.; Lee, D. H.; Kwon, M. S.; Choi, J. M.; Wu, J.; Dou, S. K.; Chang, H.; Park, W. I.; *et al.* Arrays of Sealed Silicon Nanotubes as Anodes for Lithium Ion Batteries. *Nano Lett.* **2010**, *10*, 1710–1716.
11. Choi, N.-S.; Yao, Y.; Cui, Y.; Cho, J. One Dimensional Si/Sn-Based Nanowires and Nanotubes for Lithium-Ion Energy Storage Materials. *J. Mater. Chem.* **2011**, *21*, 9825–9840.
12. Szczeh, J. R.; Jin, S. Nanostructured Silicon for High Capacity Lithium Battery Anodes. *Energy Environ. Sci.* **2011**, *4*, 56–72.
13. Braun, P. V.; Cho, J.; Pikul, J. H.; King, W. P.; Zhang, H. High Power Rechargeable Batteries. *Curr. Opin. Solid State Mater. Sci.* **2012**, *16*, 186–198.
14. Huang, R.; Fan, X.; Shen, W.; Zhu, J. Carbon-Coated Silicon Nanowire Array Films for High-Performance Lithium-Ion Battery. *Appl. Phys. Lett.* **2009**, *95*, 133119.
15. Hertzberg, B.; Alexeev, A.; Yushin, G. Deformations in Si-Li Anodes Upon Electrochemical Alloying in Nano-Confined Space. *J. Am. Chem. Soc.* **2010**, *132*, 8548–8549.
16. McDowell, M. T.; Lee, S. W.; Wang, C.; Cui, Y. The Effect of Metallic Coatings and Crystallinity on the Volume Expansion of Silicon During Electrochemical Lithiation/Delithiation. *Nano Energy* **2012**, *1*, 401–410.
17. Sethuraman, V. A.; Kowolik, K.; Srinivasan, V. Increased Cycling Efficiency and Rate Capability of Copper-Coated Silicon Anodes in Lithium-Ion Batteries. *J. Power Sources* **2011**, *196*, 393–398.
18. Sandu, I.; Brousse, T.; Schleich, D. M. Effect of Nickel Coating on Electrochemical Performance of Graphite Anodes for Lithium Ion Batteries. *Ionics* **2003**, *9*, 329–335.
19. Subramanian, V. R.; Yu, P.; Popov, B. N.; White, R. E. Modeling Lithium Diffusion in Nickel Composite Graphite. *J. Power Sources* **2001**, *96*, 396–405.
20. Yu, Y.; Gu, L.; Zhu, C.; Tsukimoto, S.; van Aken, P. A.; Maier, J. Reversible Storage of Lithium in Silver-Coated Three-Dimensional Macroporous Silicon. *Adv. Mater.* **2010**, *22*, 2247–2250.
21. Xiao, X.; Lu, P.; Ahn, D. Ultra Multifunctional Oxide Coatings for Lithium Ion Batteries. *Adv. Mater.* **2011**, *23*, 3911–3915.
22. Yao, Y.; McDowell, M. T.; Ryu, I.; Wu, H.; Liu, N.; Hu, L.; Nix, W. D.; Cui, Y. Interconnected Silicon Hollow Nanospheres for Lithium-Ion Battery Anodes with Long Cycle Life. *Nano Lett.* **2011**, *11*, 2949–2954.
23. Ghassemi, H.; Au, M.; Chen, N.; Heiden, P. A.; Yassar, R. S. *In Situ* Electrochemical Lithiation/Delithiation Observation of Individual Amorphous Si Nanorods. *ACS Nano* **2011**, *5*, 7805–7811.
24. Wu, H.; Chan, G.; Choi, J. W.; Ryu, I.; Yao, Y.; McDowell, M. T.; Lee, S. W.; Jackson, A.; Yang, Y.; Hu, L.; *et al.* Stable Cycling of Double-Walled Silicon Nanotube Battery Anodes through Solid-Electrolyte Interphase Control. *Nat. Nanotechnol.* **2012**, *7*, 309–314.
25. Wang, J. W.; He, Y.; Fan, F.; Liu, X. H.; Xia, S.; Liu, Y.; Harris, C. T.; Li, H.; Huang, J. Y.; Mao, S. X.; *et al.* Two-Phase Electrochemical Lithiation in Amorphous Silicon. *Nano Lett.* **2013**, *13*, 709–715.
26. McDowell, M. T.; Lee, S. W.; Harris, J. T.; Korgel, B. A.; Wang, C.; Nix, W. D.; Cui, Y. *In Situ* TEM of Two-Phase Lithiation of Amorphous Silicon Nanosphere. *Nano Lett.* **2013**, *13*, 758–764.
27. Karki, K.; Epstein, E.; Cho, J-H; Jia, Z.; Li, T.; Picraux, S. T.; Wang, C.; Cumings, J. Lithium-Assisted Electrochemical Welding in Silicon Nanowire Battery Electrodes. *Nano Lett.* **2012**, *12*, 1392–1397.
28. Sun, C.-F.; Karki, K.; Jia, Z.; Liao, H.; Zhang, Y.; Li, T.; Qi, Y.; Cumings, J.; Rubloff, G. W.; Wang, Y. A Beaded-String Silicon Anode. *ACS Nano* **2013**, *7*, 2717–2724.
29. Abel, P. R.; Lin, Y.-M.; Celio, H.; Heller, A.; Mullins, C. B. Improving the Stability of Nanostructured Silicon Thin Film Lithium-Ion Battery Anodes through Their Controlled Oxidation. *ACS Nano* **2012**, *6*, 2506–2516.
30. Yang, J.; Takeda, Y.; Imanishi, N.; Capiglia, C.; Xie, J. Y.; Yamamoto, O. SiO_x-Based Anodes for Secondary Lithium Batteries. *Solid State Ionics* **2002**, *152−153*, 125–129.
31. Kim, K.; Park, J.-H.; Doo, S.-G.; Kim, T. Effect of Oxidation on Li-Ion Secondary Battery with Non-Stoichiometric Silicon Oxide (SiO_x) Nanoparticles Generated in Cold Plasma. *Thin Solid Films* **2010**, *518*, 6547–6549.
32. Sun, Q.; Zhang, B.; Fu, Z. Lithium Electrochemistry of SiO_2 Thin Film Electrode for Lithium-Ion Batteries. *Appl. Surf. Sci.* **2008**, *254*, 3774–3779.
33. Wang, J. W.; Liu, X. H.; Zhao, K.; Palmer, A.; Patten, E.; Burton, D.; Mao, S. X.; Suo, Z.; Huang, J. Y. Sandwich-Lithiation and Longitudinal Crack in Amorphous Silicon Coated on Carbon Nanofibers. *ACS Nano* **2012**, *6*, 9158–9167.
34. Liu, X. H.; Zheng, H.; Zhong, L.; Huang, S.; Karki, K.; Zhang, L. Q.; Liu, Y.; Kushima, A.; Liang, W. T.; Wang, J. W.; *et al.* Anisotropic Swelling and Fracture of Silicon Nanowires during Lithiation. *Nano Lett.* **2011**, *11*, 3312–3318.
35. Wang, C.-M.; Li, X.; Wang, Z.; Xu, W.; Liu, J.; Gao, F.; Kovarik, L.; Zhang, J.-G.; Howe, J.; Burton, D. J.; *et al. In Situ* Investigation of Congruent Phase Transition and Structural Evolution of Nanostructured Silicon/Carbon Anode for Lithium Ion Batteries. *Nano Lett.* **2012**, *12*, 1624–1632.
36. Zhao, K.; Pharr, M.; Hartle, L.; Vlassak, J. J.; Suo, Z. Fracture and Debonding in Lithium-Ion Batteries with Electrodes of Hollow Core-Shell Nanostructures. *J. Power Sources* **2012**, *218*, 6–14.
37. Zhang, S.; Du, Z.; Lin, R.; Jiang, T.; Liu, G.; Wu, X.; Weng, D. Nickel Nanocone-Array Supported Silicon Anode for High-Performance Lithium-Ion Batteries. *Adv. Mater.* **2010**, *22*, 5378–5382.
38. Deal, B. E.; Grove, A. S. General Relationship for the Thermal Oxidation of Silicon. *J. Appl. Phys.* **1965**, *36*, 3770–3778.